ELSEVIER

Dyes and Pigments, Vol. 38, Nos 1–3, pp. 77–95, 1998

Printed in Great Britain
PII: S0143-7208(97)00110-1 0143-7208/98 $19.00+0.00

Synthesis of a Bioactive Fluorescent Dye and Enzymatic Labeling at the 3-termini of RNAs: An Application for the Characterization of the Thermal Stability of tRNAs and Oligonucleotides Using Fluorescence Anisotropy Measurements

Masataka Kinjo,* Tsunehisa Araiso† & Tomiyasu Koyama

Research Institute for Electronic Science, Hokkaido University, Sapporo, 060, Japan

(Received 13 October 1997; accepted 12 November 1997)

ABSTRACT

A novel fluorescent nucleotide analogue, 2'-O-anthraniloylcytidine 3',5'-diphosphate (Ant-pCp) was synthesized from cytidine 3',5'-diphosphate and isatoic anhydride. Using T4 RNA ligase, Ant-pCp was easily joined to the 3' terminus of the various oligonucleotides and tRNAs, for example, $(pA)_4$, $(pA)_6$, $(pA)_8$, yeast $tRNA^{Phe}$, B. subtilis *$tRNA^{Thr}$, and* B. subtilis *unfractionated tRNA. It seems that anthraniloyl group does not influence the ligation reaction. Steady-state fluorescence anisotropy (r^s) of these labeled oligonucleotides or tRNAs were measured in the presence or absence of Mg^{2+} in the temperature range 5 to 60°C. The complex formation between fluorescent labeled oligonucleotides and poly(U) and the thermal denaturation profiles of the complexes were successfully detected by fluorescence anisotropy at low nucleotide concentration (10^{-6} M) in the presence of $MgCl_2$. Fluorescent labeled tRNA showed characteristic thermal denaturation profiles in the absence of Mg^{2+}, indicating that tRNA has a secondary and/or tertiary structure. The anisotropy values of the fluorescent probe decreased in the order: oligo(A):poly(U) complex > tRNA ($+Mg^{2+}$) > oligo(A). These results indicate that the mobility of the 3' terminal of tRNA is more restricted than that of the single strand of oligo(A) in solution.* © *1998 Elsevier Science Ltd. All rights reserved*

Keywords: anthranilic acid, anthraniloyl, conformation change, oligonucleotide, tRNA, RNA ligase.

*Corresponding author. Fax: +81 11706 4964; e-mail: kinjo@imdes.hokudai.ac.jp
†Present address: Center for Advanced Science and Technology, Hokkaido University, Sapporo, 060 Japan.

ABBREVIATIONS

Ant: Anthraniloyl
Ant-pCp: 2′-O-anthraniloylcytidine 3′, 5′-diphosphate
Ant-tRNA: tRNA molecules of which 3′-terminal have been ligated with Ant-pCp
CTABr: Cetyltrimethylammonium bromide
DMF: N,N-Dimethylformamide
IA: Isatoic anhydride
$(pA)_4$: $pAAAA_{OH}$
$(pA)_6$: $pAAAAAA_{OH}$
$(pA)_8$: $pAAAAAAAA_{OH}$
$pAAAACp^{Ant}$: $(pA)_4$ molecules of which 3′-terminal have been ligated with Ant-pCp
pCp: Cytidine 3′, 5′-diphosphate
Et_3N: Triethylammonium
One A_{260} unit is defined as an amount of material which gives an absorbance of 1.0 at 260 nm when dissolved in 1 ml water and measured with a 1 cm light path
Enzyme: T4 RNA ligase (EC 6.5.1.3.)

INTRODUCTION

Specific interaction between an amino acid and its cognate tRNA is performed by the corresponding aminoacyl tRNA synthetase. Many parameters affect the efficiency of aminoacylation of tRNA [1, 2]. The minimum nucleotide sequence required to be recognized as a substrate for alanyl tRNA synthetase was constructed with a six nucleotides loop and an amino acid acceptor end [3]. Anticodon sequence is also an important parameter in this reaction in whole structured tRNA. It is evident that a specific structure in tRNA is required for aminoacylation. Various techniques can be applied in order to detect tRNA structural changes upon amino acid recognition of tRNA [4, 5]. Among those methods, fluorescence depolarization has become a powerful tool for the study of the flexibility and rigidity of macromolecules [6–8]. Unfortunately, few attempts have been made to obtain information about tRNA structure using fluorescence intensity [9–12] and fluorescence depolarization measurements [13–17]. In these works, two fluorophores were used. One was Y-base, an intrinsic fluorescent nucleotide found exclusively 3′, adjacent to the anticodon of most eukaryotic $tRNA^{Phe}$, and another was the modified s^4U_8 found in many prokaryotic tRNAs. Thus, these fluor-

ophores could be used in only a limited variety of organisms and tRNA species, resulting in limited information about tRNA structure by their fixed position. T4 RNA ligase was found to be useful for the synthesis of oligodeoxyribonucleotide containing fluorescent nucleotide analogues [18, 19] and the synthesis of $tRNA^{Phe}$ containing fluorescent analogues [20–22]. T4 RNA ligase also has been used as a valuable tool for the synthesis of single stranded oligoribonucleotides [23–25] and for the alteration of the sequence of the anticodon of $tRNA^{Phe}$ [26–28], $tRNA_f^{Met}$ [29, 30], $tRNA^{Thr}$ [31] and alteration of the loop of $tRNA^{Tyr}$ [32].

It has been reported that anthraniloyl groups have high quantum yields, convenient wavelengths of absorption and emission spectra, and molecular sizes which are smaller than most fluorophores that had been previously used for fluorescent labeling to ATP [33]. Thus, anthraniloyl groups have been described not only as a good substrate for some enzymes [34–37] but also as labeling reagents for HPLC [38].

In the present work, we have synthesized a new fluorescent nucleotide analogue which could serve as a substrate for T4 RNA ligase, and we have employed this enzyme to label oligonucleotides and tRNAs fluorescently. Fluorescence anisotropy changes in labeled oligonucleotides and tRNA were studied in order to obtain structural information of the nucleotide strands.

MATERIALS AND METHODS

Chemicals

Cytidine 3′,5′-diphosphate (pCp) was purchased from Pharmacia. Poly(U) was from Yamasa Shoyu Co. Isatoic anhydride was from Molecular Probes Co. T4 RNA ligase was from Takara Shuzo Co. The preparation of $pAAAA_{OH}$ [$(pA)_4$], $pAAAAAA_{OH}$ [$(pA)_6$], $pAAAAAAAA_{OH}$ [$(pA)_8$] and *Bacillus subtilis* $tRNA^{Thr}$ has been reported previously [39, 40]. Yeast $tRNA^{Phe}$ was purchased from Boehringer Mannheim GmbH. Ant-ATP was synthesized according to the literature [33]. Purity of the synthesized Ant-ATP was confirmed by thin layer chromatography. Other reagents were of analytical grade.

Chromatography

Thin layer chromatography was performed on silica-gel plates (silica-gel 60 W, Merck) in *n*-propanol–NH_4OH–H_2O (6:3:1) containing EDTA (0.5 g $litre^{-1}$) [33]. HPLC was performed on a Jasco Tri Rotor V liquid chromatograph equipped with a 6×250 mm ODS–AQ column (YMC, Japan) at room

temperature. The nucleotide analogue was purified by linear gradient elution with 0.1 M triethylammoniumacetate from 0 to 10% acetonitrile in 20 min at a flow rate of 1 ml min^{-1}. The eluate was monitored by UV absorption at 260 nm.

Synthesis

The anthraniloyl derivative of pCp was synthesized by modification of a previously reported method [33]. Thus, pCp (20 μmol) was dissolved in 25% aq. DMF (440 μl) containing 46 mM cetyltrimethylammonium bromide (CTABr) and 2.3 mM NaOH (unless otherwise stated). Isatoic anhydride (30 μmol) was dissolved in 20 μl DMF and then was added to the pCp solution. After incubation at room temperature for 18 h in the dark, the reaction mixture was checked by TLC. Cold acetone (5 μl) was added to the reaction mixture which was stored at −20°C overnight, and the precipitate was collected by centrifugation (4000 rpm, 15 min). The precipitate was washed with cold acetone. The product was then dissolved in 200 μl water and purified by HPLC, and the fraction of Ant-pCp was then evaporated. The residue was dissolved in a water and stored at −80°C until use. Each peak was checked by TLC on silica–gel. The Rf values of pCp in silica–gel were 0.07, Ant-pCp 0.12 and anthranilic acid 0.61. Purity was confirmed by elementary analysis. When the synthesis was carried out on small scale (pCp 800 nmol in Fig. 1), the reaction mixture was purified by TLC. The fluorescent spot of Ant-pCp was scraped from the plate and eluted from the silica gel with water. The concentration of fluorescent labeled RNA was determined using $E_{332} = 4700\ M^{-1}\ cm^{-1}$ for the anthraniloyl group [33]; chemical structure was characterized by 500 MHz H-NMR in D_2O.

Reaction with RNA ligase

The synthesis of fluorescent labeled oligo(A)s and tRNAs was adapted from the previously described oligo RNA synthesis [40, 41]. The ligation was carried out with 5 μl of reaction mixture containing 50 mM Hepes-NaOH (pH 8.3), 20 mM $MgCl_2$, 5 mM dithiothreitol, 10 $\mu g\,ml^{-1}$ bovine serum albumin, 10% dimethyl-sulfoxide, 0.8 mM oligo(A) or 1 A_{260} unit of tRNA as acceptor, 1.1 mM Ant-pCp as donor, 2.5 mM ATP and 25 units of T4 RNA ligase. The reaction mixture was incubated at 4°C for 18 h in the dark. The products of ligation were separated by 10% polyacrylamide gel electrophoresis which contained 0.089 M Tris base, 0.089 M boric acid and 0.002 M sodium EDTA and 7 M urea [42].

tRNA and oligo(A) were detected by UV monitoring (254 nm) [43]. Fluorescence on gel was detected using a transmission UV lamp (315 nm)

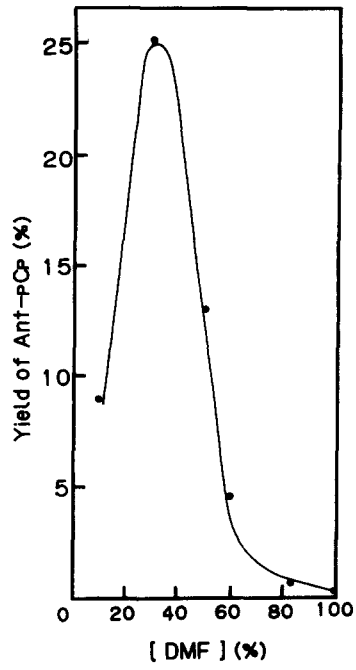

Fig. 1. Yield of Ant-pCp as a function of concentration of DMF. The reaction mixture (10 μl) contained pCp 800 nmol, isatoic anhydride 3 mmol, CTABr 800 nmol, NaOH 100 nmol and DMF. Reaction and TLC separation condition were as described in the Materials and Methods section. Each spot (Rf = 0.12) was scraped and immersed in H_2O. After silica-gel was removed by centrifugation, the fluorescence intensity was measured.

and PO1 and Y2 filters which were equipped in this order from outside the camera lens. The labeled and non-labeled RNA bands were cut out and immersed in 0.5 ml of 10 mM Tris-HCl (pH 7.4) at 4°C for 2 h in the dark. The solutions were filtered through a cellulose acetate membrane (0.22 mm. Spinx, Corstar.) by centrifugation on the original gel. The extraction procedure was repeated 3 times. The total eluant (2 ml) was collected for fluorescence anisotropy measurement.

Fluorescence anisotropy and UV measurement

The steady-state fluorescence anisotropy (r^s) was measured using a Shimadzu-RF 540 spectrofluorophotometer equipped with polarizers (P/N-204-03290-01), and is defined by the equation:

$$r^s = (I_{VV} - f \cdot I_{VH})/(I_{VV} + 2f \cdot I_{VH})$$

where I_{VV} and I_{VH} are observed intensity measured with the polarizers parallel and perpendicular to the vertically polarized excitation beam. The correction factor, $f = I_{HV}/I_{HH}$, represents the ratio of fluorescence intensity with the polarizers perpendicular and parallel to the horizontally polarized excitation beam. The excitation and emission wavelengths were 340 nm and 430 nm, respectively. Slits of 10 nm in width were set in the excitation and emission light paths in all measurements. The intensity (I_{VV}, I_{VH}, I_{HH}, I_{HV}) of labeled RNA used was obtained after subtracting the intensity of non-labeled RNA from the raw intensity of labeled RNA under the same conditions. UV absorption profiles were measured 260 nm.

All thermal denaturation profiles were measured in 10 mM Tris–HCl (pH 7.4) and in the presence of 10 mM $MgCl_2$ (or in the absence of $MgCl_2$). For each determination, the samples were heated at 60°C for 10 min, and then allowed to cool slowly, first to 45°C over a period of 30 min and to the starting temperature (usually 5°C). The temperature was raised at 5°C 15 min^{-1}.

RESULTS

Characterization

The chemical structure of the new fluorescent derivative of cytidine 3′,5′-diphosphate is shown in Fig. 2. Attachment of the anthranilic acid moiety to pCp is simple, and is a one-step reaction. The reaction mixture necessarily contained quaternary ammonium ion (cetyltrimethylammonium) and DMF.

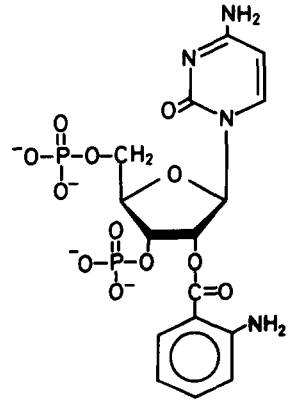

Fig. 2. Chemical structure of Ant-pCp.

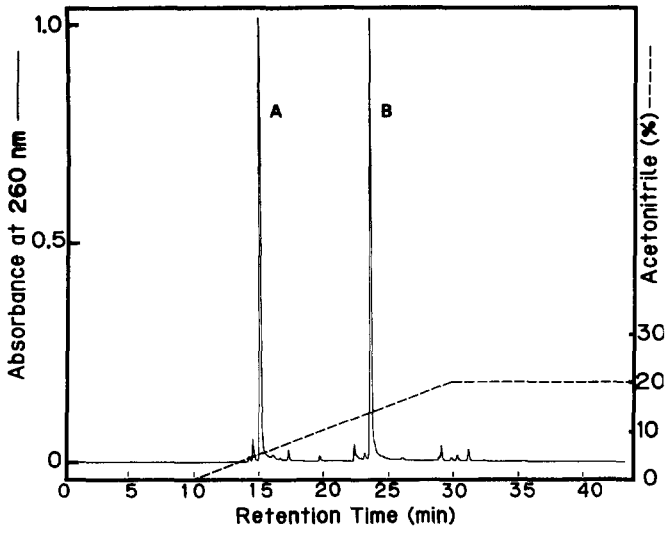

Fig. 3. Results of HPLC purification of chemically synthesized Ant-pCp. Reaction conditions were as described in the Materials and Methods section. After washing the reaction products of pCp and isatoic anhydride with cold acetone, the precipitate was dissolved in H_2O (200μl) and then an aliquot was applied to an ODS column. Elution was carried out with a gradient of acetonitrile (- - -) over 20 min. Peaks A and B are due to pCp and Ant-pCp, respectively.

When these were omitted, the yield was found to be only 0.01%. Maximum yield was about 25% in the presence of 30% DMF and 0.08 M cetyltrimethylammonium bromide (Fig. 1). The reaction product was purified by HPLC equipped with a gradient system. The fluorescent analogue eluted after the unreacted mononucleotide (Fig. 3) and its purity was established by TLC and elementary analysis. Ant-pCp$(Et_3N)_4 \cdot 3H_2O$ (981.28) $C_{40}H_{80}N_8O_{12}P_2 \cdot 3H_2O$, calc. C 48.96% H 8.85% N 11.42% found C 49.30% H 8.53% N 10.99%.

The chemical structure of Ant-pCp was also established by H-NMR and COSY, which showed that the anthraniloyl group does not attach to the NH_2 of the base, but attaches to the OH of the sugar moiety. Fluorescence excitation and emission spectra of Ant-pCp and Ant-ATP are shown in Fig. 4. The excitation spectra in the wavelength region below 280 nm were affected by the nature of the particular nucleotide base. The emission spectra were centered at about 430 nm and corresponded to an anthraniloyl group. In the fluorescence intensity, twice as much Ant-pCp (2 mM) as Ant-ATP (1 mM) had a less intense spectrum and this lower intensity could be explained by the presence of the 3′-phosphate moiety because of which the fluorescence intensity was increased by alkaline phosphatase treatment (data not shown).

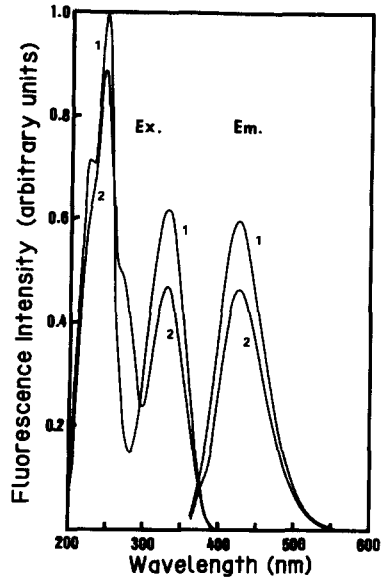

Fig. 4. The excitation (Ex) and emission (Em) spectra of nucleotide derivative. 1. Ant-ATP 1 μM; 2. Ant-pCp 2 μM. Both samples were measured in 10 mM Tris–HCl (pH 7.4) at 20°C The excitation spectrum measurements were made at emission wavelength 425 nm,and the emission spectrum measurements were made at excitation wavelength at 330 nm.

Addition of Ant-pCp to Oligo(A)s

The procedure used in the joining of oligo(A) and tRNA to label them with Ant-pCp is outlined in Fig. 5. The labeled oligonucleotide were elongated by one nucleotide long, compared with the starting material used in the ligase reaction. The fluorescent analogue, Ant-pCp, was used as the donor for T4 RNA ligase and the products of the ligation step were separated by polyacrylamide gel electrophoresis (Fig. 6(A) and (B)). The location of Ant-pCp labeled oligo(A) can be conveniently detected with its greenish-blue fluorescence after separation by polyacrylamide gel electrophoresis [Fig. 6(B) lines 2, 4, 6]. Detection of starting materials with UV lamp showed a single band and therefore minor bands were explained by backward reaction of ligase. The fluorescent labeled pentanucleotide, $pAAAACp^{Ant}$ moved faster than $pAAAA_{OH}$ (Fig. 6(A) line 1, (B) line 2) but slower than the non-labeled pentanucleotide, pAAAACp (data not shown). This result could be due to the fact that pAAAACp has a larger negative charge than pAAAA.

Mobility on the gel decreased in the order $pAAAACp > pAAAACp^{Ant} > pAAAA_{OH}$. In the largest molecule, $(pA)_8$, this difference of mobility is decreased (Fig. 6 lines 3–6). The yield of the ligation, as determined from the gel extract, was about 23% for $(pA)_4$, 46% for $(pA)_6$ and 57% for $(pA)_8$. The

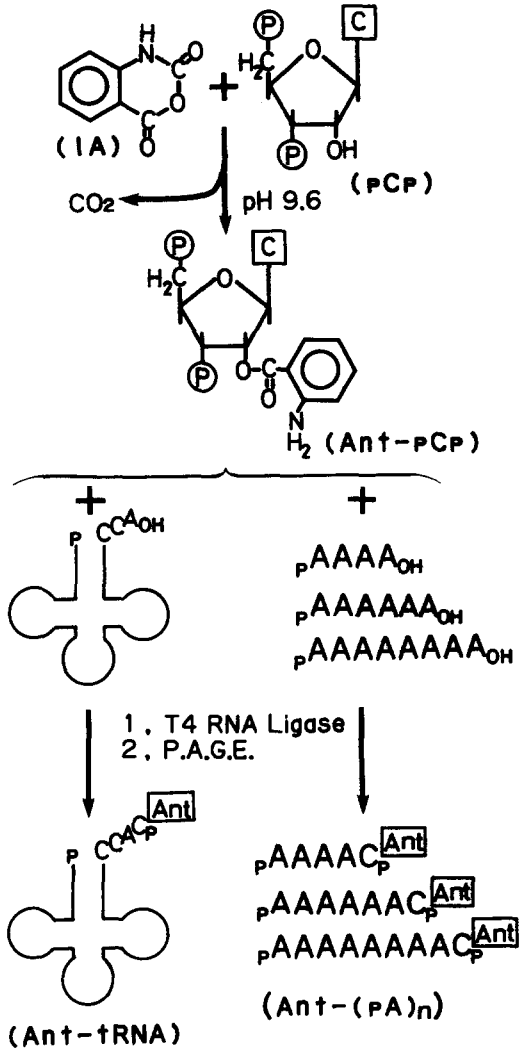

Fig. 5. Outline of the procedure used for enzymatic synthesis of Ant-tRNA and Ant-(pA)n.

apparent fluorescence spectrum of anthraniloyl labeled oligo(A) (data not shown) was similar to the subtracted fluorescence spectra of labeled tRNA (see below).

Addition of Ant-pCp to tRNAs

The greenish-blue fluorescence band (Fig. 7(B) lines 2 and 4) was superimposable on the UV absorption band (Fig. 7(A) lines 2 and 4). This fluorescent band (Fig. 7 lines 2 and 4) migrated the same distance as non-labeled tRNA (Fig. 7(A) lines 1 and 3). Fluorescent labeled and non-labeled

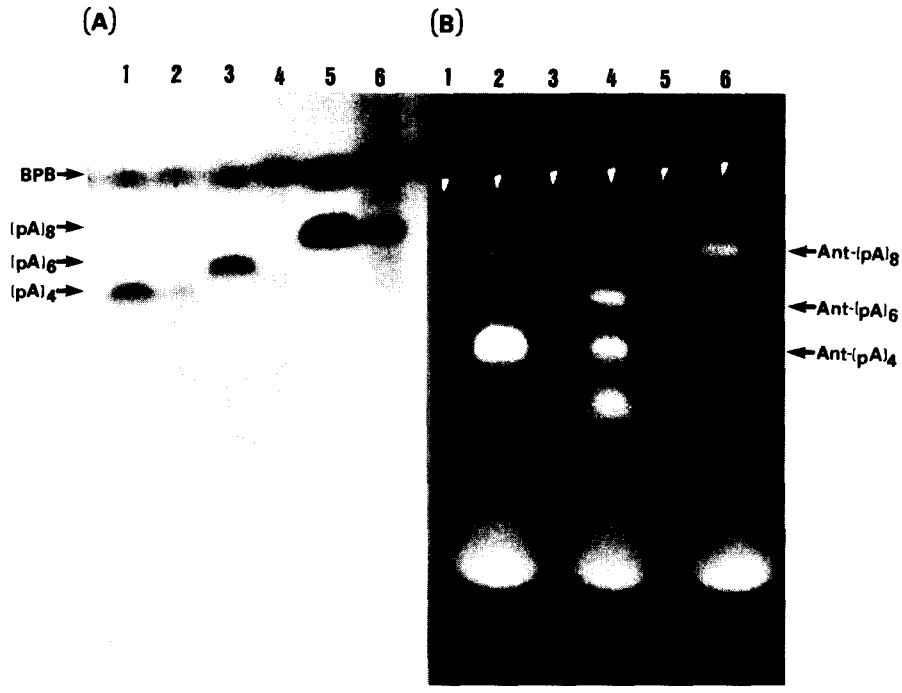

Fig. 6. T4 RNA ligase reaction with oligo(A) and Ant-pCp analyzed by 10% polyacrylamide gel electrophoresis. The reactions were performed as described in the Materials and Methods section with 0.8 mM oligo(A), 1.1 mM Ant-pCp and 25 units of T4 RNA ligase. (A) UV absorption bands were detected on a silica–gel F TLC plate under illumination with UV-lamp (254 nm); (B) fluorescence bands were detected on a transilluminator (365 nm); 1, $(pA)_4$; 2, ligation of $(pA)_4$ and Ant-pCp; 3, $(pA)_6$; 4, ligation of $(pA)_6$ and Ant-pCp; 5, $(pA)_8$; 6, ligation of $(pA)_8$ and Ant-pCp. The location of the dye bromophenol blue (BPB) is indicated by arrow and small triangles.

unfractionated tRNA had the same behavior as that found in other tRNA, except that the band was smeared and that 5S RNA was observed (Fig. 7(A) lines 5 and 6). The average yield of the ligation products, as determined from the gel extract, was about 30%. Fluorescence spectra of Ant labeled *B. subtilis* unfractionated tRNA, $tRNA^{Thr}$ and yeast $tRNA^{Phe}$ which were extracted from the polyacrylamide gel are shown in Fig. 8. Apparent fluorescence spectra of unfractionated tRNA and $tRNA^{Thr}$ extracted from gel were similar, whereas apparent fluorescence spectra of $tRNA^{Phe}$ were different from the others. This intrinsic fluorescence of $tRNA^{Phe}$ is due to Y-base, which is found 3′ adjacent in the anticodon. However, the spectra, after subtracting those of non-labeled tRNAs, showed a similar shape for all three fluorescent labeled tRNAs (Fig. 8(A2), (B2) and (C2)). Excitation spectra centered at about 340 nm, and emission spectra centered at about 430 nm, for these three

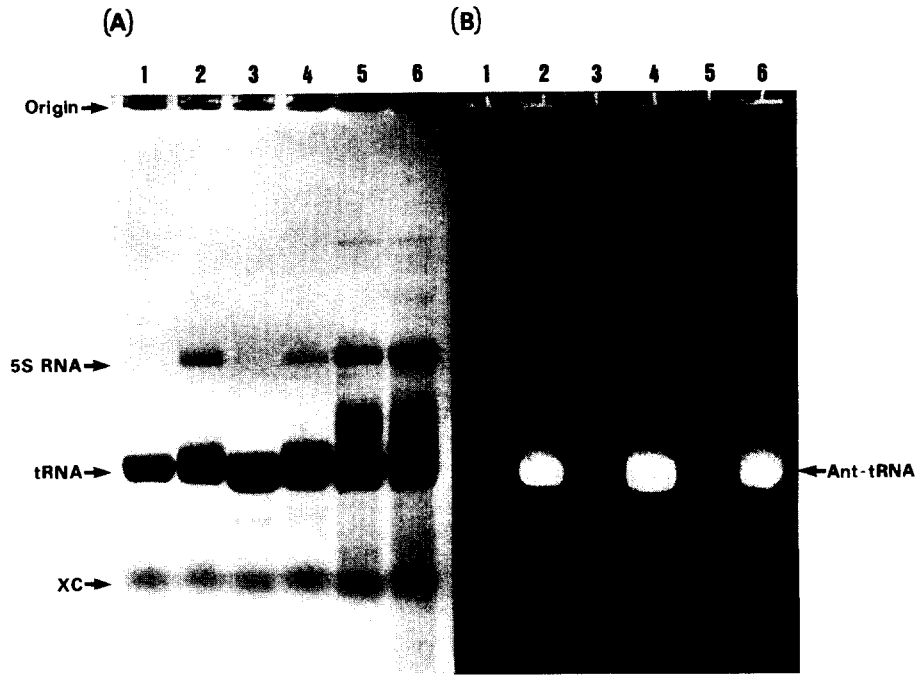

Fig. 7. T4 RNA ligase reaction with tRNA and Ant-pCp analyzed by 10% polyacrylamide gel electrophoresis. The reactions were performed as described in the Materials and Methods section with tRNA $1A_{260}$ unit, 1.1 mM Ant-pCp and 25 units of T4 RNA ligase. (A) UV shadow; (B) fluorescence emission; 1, yeast $tRNA^{Phe}$; 2, ligation of yeast $tRNA^{Phe}$ and Ant-pCp; 3, *B. subtilis* $tRNA^{Thr}$; 4, ligation of *B. subtilis* $tRNA^{Thr}$ and Ant-pCp; 5, unfractionated *B. subtilis* tRNA; 6, ligation of unfractionated *B. subtilis* tRNA and Ant-pCp. The location of the dye xylene cyanol FF (XC) is indicated by an arrow.

subtracted fluorescence spectra mirrored one another. The subtracted fluorescence intensity was used for the fluorescence anisotropy calculation.

Thermal denaturation profile of fluorescence anisotropy and UV absorption of Ant-oligo(A)

The effect of temperature on the fluorescence anisotropy of oligo(A) was investigated in the presence of both $MgCl_2$ and poly(U). In the absence of either $MgCl_2$ or poly(U), with the other being present, fluorescence anisotropy gradually decreased with increasing temperature (Fig. 9. open symbols) and no melting curve was generally apparent. In the presence of both $MgCl_2$ and poly(U) a thermal denaturation profile was obtained. Melting temperature depended on the chain length of oligo(A). The apparent T_m, from fluorescence anisotropy and UV absorption measurements, was 9°C for Ant-$(pA)_4$, 34.3°C for Ant-$(pA)_6$, and 43.7°C for Ant-$(pA)_8$.

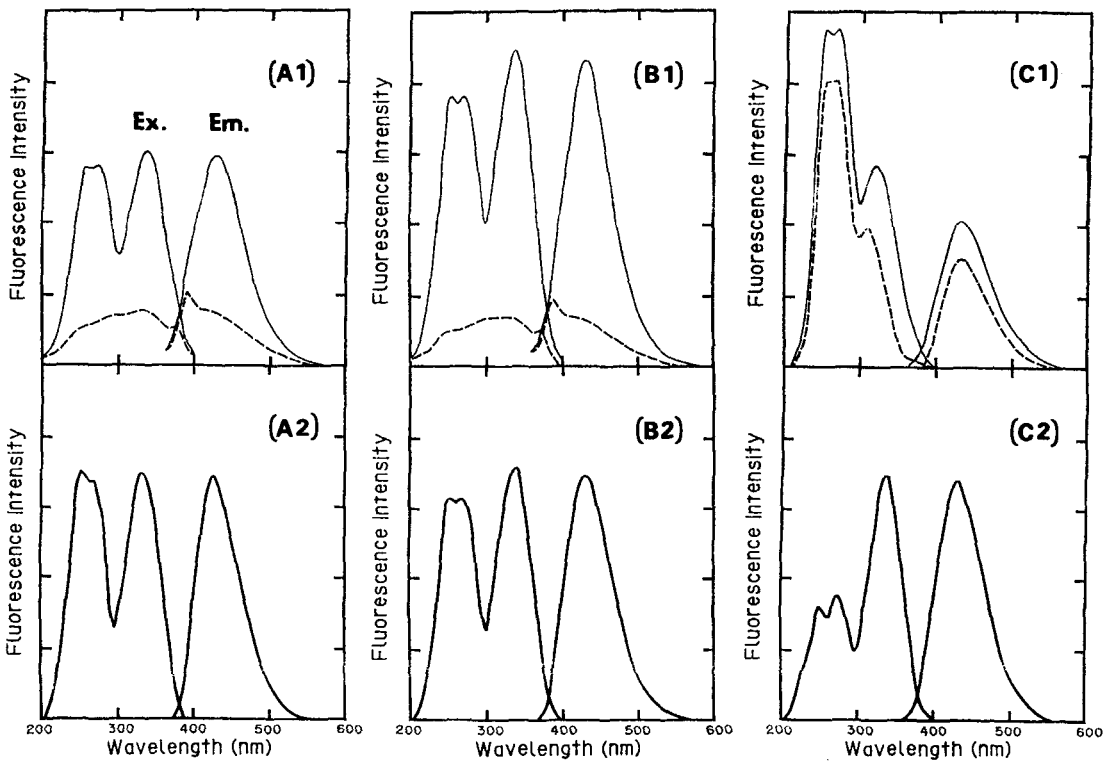

Fig. 8. The excitation (Ex) and emission (Em) spectra of the ligation products of Ant-pCp to tRNA. Fluorescent labeled and non-labeled tRNA were extracted from the gel (Fig. 7) and soaked in 2 ml of 10 mM Tris–HCl (pH 7.4) at 4°C. The excitation measurements were made at emission wavelength 430 nm, and the emission measurements were made at excitation wavelength at 340 nm at 5°C. Upper section: A1, fluorescently labeled unfractionated *B. subtilis* tRNA (—) and non-labeled unfractionated *B. subtilis* tRNA (- - -); B1, fluorescently labeled *B. subtilis* $tRNA^{Thr}$ (—) and non-labeled *B. subtilis* (- - -); C1, fluorescently labeled yeast tRNAPhe (—) and non-labeled yeast $tRNA^{Phe}$(- - -). Lower section: correct spectra with non-labeled tRNA (- - -) subtracted from that of labeled tRNA (—), shown in upper section fluorescence.

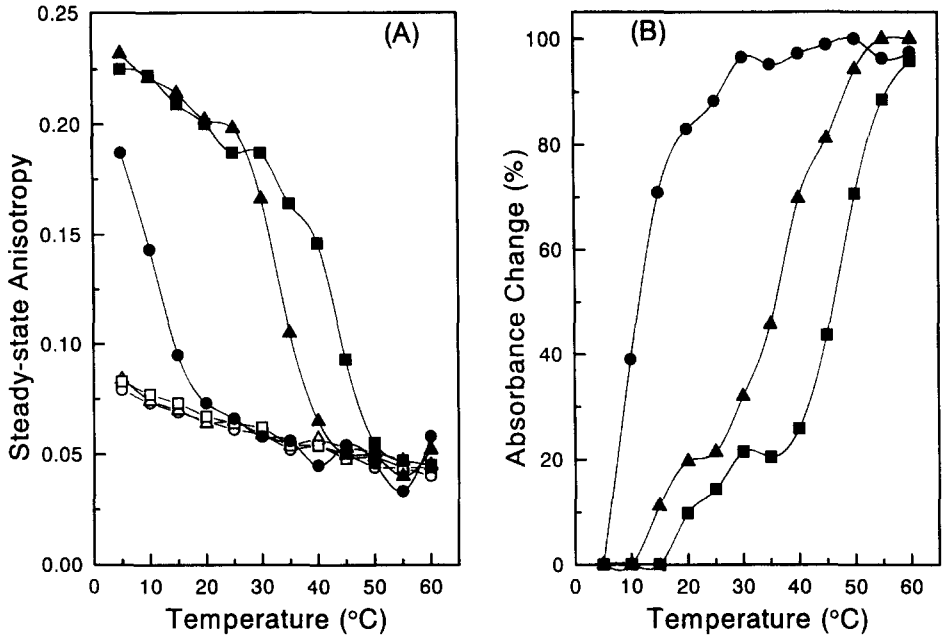

Fig. 9. Fluorescence anisotropy (A) and UV absorption (B) of the labeled oligo(A) as a function of temperature. Thermal denaturation profiles were determined as described in the Materials and Methods section. Labeled oligo(A)s were extracted from the gel (Fig. 6) and soaked in 2 ml of 10 mM Tris–HCl (pH 7.4) at 4°C. Open symbols indicate sample contained only either Mg^{2+} or poly(U). ○, Ant-(pA)4 + Mg^{2+}; △, Ant-$(pA)_6$ + poly(U); □, Ant-$(pA)_8$ + poly(U). Filled symbols indicate sample contained both 10 mM $MgCl_2$ and poly(U) at 50 $\mu g\,ml^{-1}$. ●, Ant-$(pA)_4$ + Mg^{2+} + poly(U); ▲, Ant-$(pA)_6$ + Mg^{2+} + poly(U); ●, Ant-$(pA)_8$ + Mg^{2+} + poly(U).

Thermal denaturation profile of fluorescence anisotropy of Ant-tRNA

The effect of temperature on the fluorescence anisotropy of tRNA was investigated in the presence or absence of $MgCl_2$ (Fig. 10). In the presence of $MgCl_2$, the present three tRNAs showed similar thermal denaturation profiles, which gradually decreased with increasing temperature. In the absence of $MgCl_2$, these three tRNAs showed different changes in fluorescence anisotropy with rise of temperature. The two melting temperatures of $tRNA^{Thr}$ were found as to be 12.5 and 45°C. Single Tm was found for unfractionated tRNA and $tRNA^{Phe}$, 50 and 35.8°C, respectively. A marked decrease in fluorescence anisotropy from 0.12 to 0.06 was observed for $tRNA^{Phe}$ around Tm, 35.8°C. At 5°C, the effect of $MgCl_2$ on the fluorescence anisotropy of tRNAs was small, the six data being distributed around 0.14. On the other hand, in the range of 35 to 60°C, fluorescence anisotropy

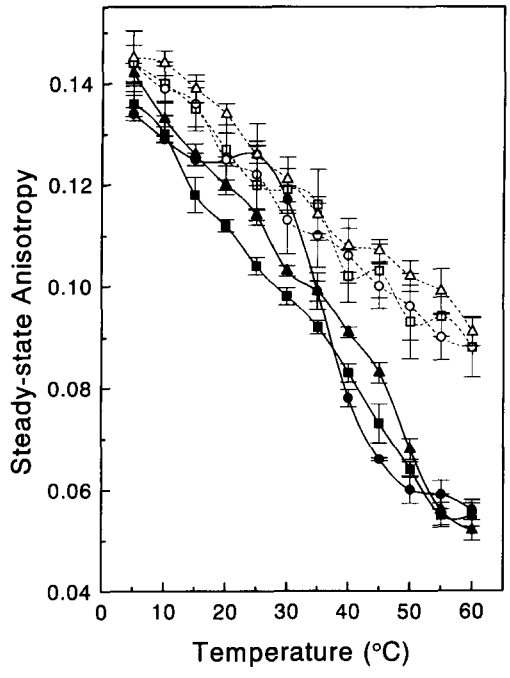

Fig. 10. Fluorescence anisotropy of the labeled tRNA as a function of temperature. Thermal denaturation profiles were determined as described in the Materials and Methods section with 10 mM Tris–HCl (pH 7.4) alone (filled symbols) or with 10 mM Tris–HCl (pH 7.4) and 10 mM $MgCl_2$ (open symbols); ▲, △, unfractionated *B. subtilis* tRNA; ■, □, *B. subtilis* $tRNA^{Thr}$; ●, ○, yeast $tRNA^{Phe}$. Shown are mean values ($n = 3$) ± S.E. (vertical bar).

of tRNAs of all three species in the absence of $MgCl_2$ became lower than that in the presence of $MgCl_2$.

DISCUSSION

Synthesis of Ant-pCp

Cetyltrimethylammonium bromide (CTABr) was very effective in increasing the yield in the synthesis of the anthraniloyl (Ant) labeled fluorescent analog of pCp. The yield of Ant-pCp was less than 1% in the absence of CTABr (data not shown). Contrary to our results, it was previously reported that isatoic anhydride (IA) reacted readily with the 2′(3′) hydroxyl group of mononucleotide triphosphate [33] and alcohols [44] in the absence of CTABr. The molecule of pCp has a large negative charge due to 3′-phosphate moiety being close to the 2′ hydroxyl group. Therefore, the very low yield without CTABr suggests that the 3′-phosphate group on pCp prevents

the reaction of IA with the 2′ hydroxyl group. The present results are consistent with the previous observation that the quaternary ammonium salt of the nucleotide is soluble in a polar organic solvent [45]. In conclusion, the relatively high yield of Ant-pCp in the presence of quaternary ammonium ion (CTABr) can be explained by the assumption that CTABr compensates the negative charge at the 3′-phosphate moiety and provides a hydrophobic environment which enhances reactivity around the 2′ hydroxyl group.

Ant-pCp as a donor of RNA ligase

T4 RNA ligase has a large tolerance for donor substrates. In general, the mononucleotide 3′,5′-diphosphates, pAp, pCp, pGp, pUp [24] and fluorescent analogues, 1,N^6-ethenoadenosine [21, 22], 2′-deoxyribonucleoside 3′,5′-diphosphate (pdNp) derivative of 2-aminopurine, 2,6-diaminopurine and N^6-methyladenine [19] were used as a donor for the RNA ligase reaction. These fluorescent analogues have modified bases and hence these analogues can affect base–base interactions. In contrast, the present results show that Ant-pCp is not modified at the base moiety, but is ligated to the 3′-terminal hydroxyl group of oligo(A), tRNA and 5S RNA by T4 RNA ligase. Thus, the final products, fluorescence labeled RNA, may be used in physicochemical studies without interfering in base–base interaction. Although the ADP fluorescent derivative (Ado-5′PP-X, X = fluorescein, tetramethyl-rhodamine) may be used as substrate with T4 RNA ligase [20], the synthesis of Ado-5′PP-X needs more chemical synthesis steps than the single step synthesis of Ant-pCp. Consequently, the synthesis of Ant-pCp is much easier than that of the alternation substrate, Ado-5′PP-X. Furthermore, from the above results we conclude that any nucleotide 3′,5′-diphosphate labeled with anthraniloyl (Ant-pNp) would substrate as a donor for T4 RNA ligase reaction.

Conformation change of Ant-labeled oligo(A) and tRNA

Fluorescence measurements are more sensitive than other physico- chemical measurements, which require a high concentration of materials [4]. The anisotropy change could be measured at a low nucleotide concentration (10^{-6} M) in the present study. Therefore, the results eliminate the effect of base stacking due to a high nucleotide concentration. Mg^{2+} stabilizes the formation of the complex between poly(U) and anthraniloyl oligo(A) (Fig. 9, filled symbols). It is consistent with general concepts that a 1:2 complex of poly(A) and poly(U) are formed in the presence of high concentrations of NaCl or a divalent cation such as Mg^{2+} [46]. In addition to the above effects, the thermal stability of the complex of oligo(A):2poly(U) increases with increase in the chain length [47]. Results from our anisotropy measurements also

showed a relationship between T_m and chain length of (pA)n (Fig. 9). T_m of (pA)n have been reported by Michelson and Monny [47] by using UV absorption. In our measurements, each T_m was shifted to lower temperature than those previously reported, viz., the T_m of $(pA)_4$ is shifted from 32.6°C to 9, $(pA)_6$ from 43.0 to 34.3 and $(pA)_8$ from 52.8 to 43.7. This difference is probably caused by the oligo nucleotide used in this experiment containing fluorescent cytidine nucleotide resulting from ligation (Fig. 5). The other possibility for the difference may be the double helical structure between oligo(A):poly(U) instead of the triple helical structure. Although there is the above difference, it can be said that the decreased anisotropy could be attributed to the increased rotational diffusion rate of the 3-terminal of the oligo nucleotide due to the dissociation of oligo(A):poly(U) complex. The lack of melting curves of oligo(A) in the absence of Mg^{2+} indicate that neither the double helical nor the triple helical complex was formed. Furthermore, anisotropy changes of oligo$(pA)_4$, oligo$(pA)_6$ and oligo$(pA)_8$ were very similar and decreased almost linearly (Fig. 9, open symbols). This indicates that when the fluorescent probes bind to a single nucleotide chain containing no base pair, the probe mobility is not limited and is independent of the size of the whole molecule. The measurement of anthraniloyl labeled tRNA showed that the value of the anisotropy in the presence of Mg^{2+} (Fig. 10, dashed lines) was larger than that in the absence of Mg^{2+} (Fig. 10, solid line). The value of the anisotropy was increased 2-fold by addition of Mg^{2+} at 60°C. These results are consistent with the concept that Mg^{2+} stabilizes the secondary and tertiary structure of tRNA. When Mg^{2+} is added to tRNA, the fluorescence anisotropy of three kinds of tRNAs decrease monotonically with the rise of temperature (Fig. 10, dashed line), i.e. no conformation change of tRNA occurs in the temperature range 5 to 60°C under these conditions. Furthermore, the anisotropy values of tRNA in the presence of Mg^{2+} (Fig. 10, dashed line) are higher than those of oligo(A)s in the absence of Mg^{2+}(Fig. 9, open symbols), but lower than those of oligo(A):poly(U) complexes in the presence of Mg^{2+} (Fig. 9, filled symbols). We conclude that the motion of the 3′-terminus of tRNA is more restricted than that of single stranded oligo(A), but is more free than that of a double or triple helix. In contrast with above results, in the absence of Mg^{2+} each tRNA has a characteristic thermal denaturation profile in solution (Fig. 10, solid lines). In the absence of Mg^{2+} the secondary or tertiary structure is unstable. Under these conditions, the secondary and tertiary structure of tRNA are easily destroyed by heat. Hence, the rigid structure of the 3′-terminus in the low temperatures range changes into a loose structure at high temperature, and this change could cause the reduced fluorescence anisotropy. The conformation change of the tRNA molecule thus seems to be monitored through the fluorescence anisotropy change of the fluorophore. Each characteristic

thermal denaturation profile in the absence of Mg^{2+} would result from the nucleotide sequence of tRNAs. When the temperature rises, the values of the anisotropy of tRNA decrease ($r^s = 0.05$) and finally become nearly equal to those of oligo(A)s ($r^s = 0.045$) in the absence of Mg^{2+}. These results suggest that at high temperature the structure of the 3′- terminal of tRNA is the same as that of dissociated oligo(A). The structure of the 3′-terminal may be a single strand and have no base pair. In conclusion, the mobility of the 3′-terminus of tRNA is more restricted than that of single-strand oligoribonucleotides in solution. This low flexibility may be necessary for the recognition of aminoacyl-tRNA synthetase and/or the other related protein. In this study, we have demonstrated that steady-state fluorescence anisotropy measurements can be successfully utilized to gain information on the dynamic structure of tRNA. The apparent mobility of the tRNA 3′-terminal measured by steady-state fluorescence anisotropy includes the rotational diffusion of the whole molecule and of the segmental mobility of aminoacyl stem. Another fluorescence labeling method of anthraniloyl group to tRNA was applied to determine the binding with elongation factor Tu [48].

The direct chemical labeling method can apply to only one portion of tRNA, such as the 3′ end. On the other hand, the T4 RNA ligase based fluorescence labeling method can be applied to a variety of RNA, such as oligo RNA to mRNA under more mild conditions. The enzymatic synthesis of the tRNA technique are well known [49–51] and recent advances in the fluorescence analytical method could open up the horizon of a new field of nucleic acid research and technology [52–54]. The combination of the above novel method for fluorescent labeling of RNA and the enzymatic synthesis of RNA could facilitate physico-chemical studies on RNA, and possibly result in wider applications in new sequencing methods.

ACKNOWLEDGEMENTS

The authors are grateful to Dr T. Hiratsuka, Department of Chemistry, Asahikawa Medical College, for helpful advice and discussions. M. K. thanks Professor A. Gräslund (University of Umea, Sweden) for NMR measurement and discussion, and Professor R. Rigler (Karolinska Institute, Sweden) for critical reading of the manuscript. The authors wish to thank also Ms Y. Hirabayashi for the typing of this manuscript. This work was partly supported by The Naito Foundation.

REFERENCES

1. Schimmel, P., *Biochemistry*, 1989, **28**, 2747–2759.

2. Pallanck, L., Pak, M. and Schulman, L. H., In *tRNA Structure, Biosynthesis, and Function*, ed. D. Söll and U. L. Raj Bandary. ASM Press Washington, DC, 1995 pp. 371–394.
3. Francklyn, C. and Schimmel, P., *Nature*, 1989, **337**, 478–481.
4. Rigler, R. and Wintermeyer, W., *Ann. Rev. Biophys. Bioeng*, 1983, **12**, 475–505.
5. Schurr, J. M., Fujimoto, B. S., Wu, P. and Song, L., In *Topics in Fluorescence Spectroscopy*, Vol. 3, ed. J. R. Lakowicz. Plenum Press, New York, 1992, pp. 137–229.
6. Lakowicz, J. R., In *Principles of Fluorescence Spectroscopy*. Plenum Press, New York, 1983, pp. 111–150.
7. Lakowicz, J. R, In *Modern Physical Methods in Biochemistry, part B*, ed. A. Neuberger and L. L. M. van Deenen. Elsevier Science Publishers, Amsterdam, 1988, pp. 1–26.
8. Steiner, R. F., In *Topics in Fluorescence Spectroscopy*, Vol. 2, ed. J. R. Lakowicz. Plenum Press, New York, 1991, pp. 1–52.
9. Bujalowski, W., Graeser, E., McLaughlin, L. W. and Porschke, D., *Biochemistry*, 1986*a*, **25**, 6365–6371.
10. Bujalowski, W., Jung, M., McLaughlin, L. W. and Porschke, *D., Biochemistry*, 1986*b*, **25**, 6372–6378.
11. Dell, V. A., Miller, D. L. and Johnson, A. E., *Biochemistry*, 1990, **29**, 1757–1763.
12. Janiak, F., Dell, V. A., Abrahamson, J. K., Watson, B. S., Miller, D. L. and Johnson, A. E., *Biochemistry*, 1990, **29**, 4268–4277.
13. Wells, B. D., *Nucleic Acid Res.*, 1984, **12**, 2157–2170.
14. Rigler, R., Claesens, F. and Kristensen, O., *Anal. Instrum.*, 1985, **14**, 525–546.
15. Claesens, F. and Rigler, R., *Eur. Biophys. J.*, 1986, **13**, 331–342.
16. Wells, B. D. and Lakowicz, J. R., *Biophys. Chem.*, 1987, **26**, 39–43.
17. Hazlett, T. L., Johnson, A. E. and Jameson, D. M., *Biochemistry*, 1989, **28**, 4109–4117.
18. Cosstick, R., McLaughlin, L. W. and Eckstein, F., *Nucleic Acids Res.*, 1984, **12**, 1791–1810.
19. Brennan, C. A. and Gumport, R. I., *Nucleic Acids Res.*, 1985, **13**, 8665–8684.
20. Richardson, R. W. and Gumport, R. I., *Nucleic Acids Res.*, 1983, **11**, 6167–6184.
21. Paulsen, H. and Wintermeyer, W., *Eur. J. Biochem.*, 1984*a*, **138**, 117–123.
22. Paulsen, H. and Wintermeyer, W., *Eur. J. Biochem,*, 1984*b*, **138**, 125–130.
23. Bruce, A. G. and Uhlenbeck, O. C., *Nucleic Acids Res.*, 1978, **5**, 3665–3677.
24. Romaniuk, E., McLaughlin, L. W., Neilson, T. and Romaniuk, P. J., *Eur. J. Biochem.*, 1982, **125**, 639–643.
25. Uhlenbeck, O. C., *Trends Biochem. Sci.*, 1983, **8**, 94–96.
26. Bruce, A. G. and Uhlenbeck, O. C., *Biochemistry*, 1982, **21**, 855–861.
27. Droogmans, L., Haumont, E., de Henau, S. and Grosjean, H., *EMBO J.*, 1986, **5**, 1105–1109.
28. Droogmans, L. and Grosjean, H., *EMBO J.*, 1987, **6**, 477–483.
29. Ohtsuka, E., Doi, T., Fukumoto. R., Matsugi, J. and Ikehara, M., *Nucleic. Acids Res.*, 1983, **11**, 3863–3872.
30. Grosjean, H., de Henau, S., Doi, T., Yamane, A., Ohtsuka, E., Ikehara, M., Beauchemin, N., Nicoghosian, K. and Cedergren, R., *Eur. J. Biochem.*, 1987, **166**, 325–332.

31. Hasegawa, T., Murao, K. and Ishikura, H., *Nucleic Acids Res.*, 1984, **15**, 121–124.
32. Ohyama, T., Nishikawa, K. and Takemura, S. J., *Biochem.*, 1985, **97**, 29–36.
33. Hiratsuka, T., *Biochim. Biophys. Acta*, 1983, **742**, 496–508.
34. Hiratsuka, T. J., *Biol. Chem.*, 1982, **257**,13354–13358.
35. Karuppiah, N. and Mutus, B., *Anal. Biochem.*, 1985, **149**, 202–208.
36. Johnson, J. D., Walters, J. D. and Mills, J. S., *Anal. Biochem.*, 1987, **162**, 291–295.
37. Labruyëre, E., Mock, M., Surewicz, W. K., Mantsch, H. H., Rose, T., Munier, H., Sarfati, R. S. and Bârzu, O., *Biochemistry*, 1991, **30**, 2619–2624.
38. Sonoki, S., Sono, Y., Hisamatsu, S. and Sugiyama, T. J., *Chromato.*, 1993, **16**, 343–352.
39. Kinjo, M., Ishigami, M., Hasegawa, T. and Nagano, K. J., *Mol. Evol.*, 1984, **20**, 59–65.
40. Kinjo, M., Hasegawa, T., Nagano, K., Ishikura, H. and Ishigami, M. J., *Mol. Evol.*, 1986, **23**, 320–327.
41. Kikuchi, Y., Hishinuma, F. and Sakaguchi, K., *Proc. Natl Acad. Sci. USA*, 1978, **75**, 1270–1273.
42. Ikemura, T. and Dahlberg, J. E., *J. Biol. Chem.*, 1973, **248**, 5024–5032.
43. Hassur, S. M. and Whitlock Jr, H. W., *Anal. Biochem.*, 1974, **59**, 162–164.
44. Staiger, R. P. and Miller, E. B. J., *Org. Chem.*, 1959, **24**, 1214–1219.
45. Aubel-Sadron, G., Beck, G. and Ebel, J. P., *Biochim. Biophys. Acta*, 1961, **53**, 11–18.
46. Stevens, C. L. and Felsenfeld, G., *Biopolymers*, 1964, **2**, 293–314.
47. Michelson, A. M. and Monny, C., *Biochim. Biophys. Acta*, 1967, **149**, 107–126.
48. Servillo, L., Balestrieri, C., Quagliuolo, L., Iorio, E. L. and Giovane, A., *Eur. J. Biochem.*, 1993, **213**, 583–589.
49. Sharmeen, L. and Taylor, J., *Nucleic Acids Res.*, 1987, **15**, 6705–6711.
50. Groebe, D. and Uhlenbeck, O. C., *Nucleic Acids Res.*, 1988, **16**, 11725–11735.
51. Groebe, D. and Uhlenbeck, O. C., *Biochemistry*, 1989, **28**, 742–747.
52. Eigen, M. and Rigler, R., *Proc. Natl Acad. Sci. USA*, 1994, **91**, 5740–5747
53. Rigler, R., *J. Biotechnol.*, 1995, **41**, 177–186.
54. Kinjo, M. and Nishimura, G., *Bioimaging*, 1997, **5**, 134–138.